JAERI-M
86-106

THE SECOND EDDY CURRENT TESTING OF ZIRCALOY TUBE SAMPLES FROM THE OECD HALDEN REACTOR PROJECT AT REACTOR FUEL EXAMINATION FACILITY, TOKAI, JAERI

July 1986

Isao OHWADA and Yasuharu NISHINO

日本原子力研究所
Japan Atomic Energy Research Institute

JAERI-Mレポートは，日本原子力研究所が不定期に公刊している研究報告書です。
入手の問合わせは，日本原子力研究所技術情報部情報資料課（〒319－11茨城県那珂郡東海村）あて，お申しこしください。なお，このほかに財団法人原子力弘済会資料センター（〒319-11茨城県那珂郡東海村日本原子力研究所内）で複写による実費頒布をおこなっております。

JAERI-M reports are issued irregularly.
Inquiries about availability of the reports should be addressed to Information Division, Department of Technical Information, Japan Atomic Energy Research Institute, Tokai-mura, Naka-gun, Ibaraki-ken 319-11, Japan.

編集兼発行　日本原子力研究所
印　　刷　日立高速印刷株式会社

JAERI-M 86-106

The Second Eddy Current Testing of Zircaloy Tube Samples from the OECD Halden Reactor Project at Reactor Fuel Examination Facility, Tokai, JAERI

Isao OHWADA and Yasuharu NISHINO
Department of Reactor Fuel Examination,
Tokai Research Establishment,
Japan Atomic Energy Research Institute
Tokai-mura, Naka-gun, Ibaraki-ken

(Received July 3, 1986)

The Reactor Fuel Examination Facility in Tokai/ JAERI (Japan Atomic Energy Research Institute) joined to the second round robin programme on eddy current test of the Halden/ IFE. In the programme, two zircaloy tube samples with some artificial defects were provided for measurements.

To clarify the locations in axial and azimuthal directions, types and dimensions of the provided artificial defects, measured signals from eddy current test were analysed in comparison with the known defects on the calibration tube. As a result, fourteen defects were determined from the measurements. Then, the location, the type and the relative dimension of them were also revealed.

The results of those eddy current test are described in this paper.

Keywords: Eddy Current Test, Zircaloy Tube, Artificial Defect, Halden Reactor Project

原研東海・燃料試験施設におけるＯＥＣＤハルデンリアクタープロジェクトによるジルカロイ管の第２回渦電流探傷試験

日本原子力研究所東海研究所実用燃料試験室
大和田　功・西野　泰治

（１９８６年７月３日受理）

原研・東海研究所の燃料試験施設は，ハルデンリアクタープロジェクトによる渦電流探傷試験に関する第２回ラウンドロビン計画に参加した。本計画においては，数個の人工欠陥が附加された２本のジルカロイ管の試料が，測定のために与えられた。

与えられた人工欠陥の軸方向，円周方向，形状および大きさを解明するために，渦電流探傷試験により測定された信号を，標準試料の明白な欠陥と比較することによって解析を行った。その結果，測定によって14個の欠陥が決定された。さらに，欠陥の位置，形状および相対的な大きさも同様に判明した。

本報告書は，これらの渦電流探傷試験結果について記述する。

東海研究所：〒319－11　茨城県那珂郡東海村白方字白根２－４

Contents

目　　次

List of tables

List of figures

1. Introduction

Reactor Fuel Examination Facility at Tokai/ JAERI participated to the second round robin for eddy current tests on the zircaloy tube samples which were provided by the Halden/ IFE.

The two zircaloy tube samples (the calibration tube and the test specimen) were arrived on February 1986.

The equipment used was equal to the first round robin case, except the size of encircling type coils and the probe type ones. The eddy current tests were performed the test specimen as well as the calibration tube. Analysis was wade for determing the axial location, type and size of artificial defects, reference to the known defects from the calibration tube by the encircling type coils. In addition, the probe type coils were also used to identify the azimuthal location of the defects.

2. Background

2.1 Equipment and test conditions

i) Manufacturer of equipment and system type

The equipment manufacturer was by Hara Electrics Co., Ltd. Yokyo, Japan. Multifrequency Eddy Current Testing System FD-2203 NGT was used.

ii) Method for sample scanning and driving speed

The tube samples were fixed to the supporting tube where the diameter in both tubes were nearly equal. The top side of the supporting tube was attached to the fuel rod driving device through the regular chuck. Outline of the multifrequency eddy current testing system is shown in Fig. 1. Details on the supporting tube and the tube sample are shown Fig. 2.

Measurements were made at a rate of 1200 mm/min through the encircling type coils.

The driving device was also used for the probe type coils scanning of the tube samples. The tube samples were lifted vertically giving azimuthal rotation. The azimuthal rotation was set to nine degree around the tube samples basing upon the zero degree orientated by the IFE.

iii) Types of coils and geometrical features

As shown in Fig. 3, the encircling type coils were composed

1. Introduction

Reactor Fuel Examination Facility at Tokai/ JAERI participated to the second round robin for eddy current tests on the zircaloy tube samples which were provided by the Halden/ IFE.

The two zircaloy tube samples (the calibration tube and the test specimen) were arrived on February 1986.

The equipment used was equal to the first round robin case, except the size of encircling type coils and the probe type ones. The eddy current tests were performed the test specimen as well as the calibration tube. Analysis was wade for determing the axial location, type and size of artificial defects, reference to the known defects from the calibration tube by the encircling type coils. In addition, the probe type coils were also used to identify the azimuthal location of the defects.

2. Background

2.1 Equipment and test conditions

i) Manufacturer of equipment and system type

The equipment manufacturer was by Hara Electrics Co., Ltd. Yokyo, Japan. Multifrequency Eddy Current Testing System FD-2203 NGT was used.

ii) Method for sample scanning and driving speed

The tube samples were fixed to the supporting tube where the diameter in both tubes were nearly equal. The top side of the supporting tube was attached to the fuel rod driving device through the regular chuck. Outline of the multifrequency eddy current testing system is shown in Fig. 1. Details on the supporting tube and the tube sample are shown Fig. 2.

Measurements were made at a rate of 1200 mm/min through the encircling type coils.

The driving device was also used for the probe type coils scanning of the tube samples. The tube samples were lifted vertically giving azimuthal rotation. The azimuthal rotation was set to nine degree around the tube samples basing upon the zero degree orientated by the IFE.

iii) Types of coils and geometrical features

As shown in Fig. 3, the encircling type coils were composed

of one excite coil and two pick up ones.

(1) The excite coil, consisting of 48 turns of 0.37 mmϕ enamel-insulated copper wire, was wound up the out side of the pick up coils.

(2) The pick up coils, consisting of 28 turns of 0.08 mmϕ enamel-insulated copper wire (axial length: 0.5 mm, average diameter of coil: 13.3 mmϕ) were co-axially arranged at an interval of 0.3 mm.

(3) The pick up coils were wound reciprocally in opposite directions as a differential type.

As shown in Fig. 4, the probe type coils were also composed of one excite coil and two pick up ones.

(1) The excite coil, consisting of 69 turns of 0.08 mmϕ enamel-insulated copper wire, was wound up the out side of the pick up coils.

(2) The pick up coils, consisting of 20 turns of 0.05 mmϕ enamel-insulated copper wire, was wound up the core.

(3) The pick up coils were in a row of the driving direction and faced on the surface of the tube samples, as a differential type.

iv) Frequencies

Frequencies were 128 kHz and 512 kHz for the encircling type coils, and 128 kHz and 1024 kHz for the probe type coils.

v) Form of output

Six signals (X1 to X3, Y1 to Y3) measured by encircling type coils were shown in the form of scanning chart, where two position makers at intervals of 1 mm and 100 mm an involved.

(1) X1: phase angle 340 degree, frequency 128 kHz.

(2) Y1: relative phase angle to X1 is -90 degree, frequency 128 kHz.

(3) X2: phase angle 100 degree, frequency 512 kHz.

(4) Y2: relative phase angle to X2 is -90 degree, frequency 512 kHz.

(5) X3: multiplication of X1 and X2 signals.

(6) Y3: multiplication of Y1 and Y2 signals.

Signals X1, Y1, X2 and Y2 were filtered frequency eliminator at the last stage of electrical amplifiers. Range of frequencies of band path filter were between 5.8 and 12.0 Hz.

Signals X3 and Y3 were used to decide the defective location with large signals.

Two pairs of signal, (X1 Y1) and (X2, Y2) obtained from defects were vectorized to know the type of defect. These were shown in the form of X-Y plotting sheet respectively.

2.2 Method of calibration

Measuring equipment was calibrated with given calibration tube. Top of the calibration tube was set to opposite side of zero degree mark at azimuthal location.

The known defects on the calibration tube were measured by using the encircling type coils. Axial location of the defects measured were similar to those informed by the IFE. Type of the defects were identified by the phase angle, except the defect No. 7.

Results of scanning at the calibration tube are shown in Fig. 5. The X-Y plottings for known defects measured by the frequencies of 128 and 512 kHz, are shown in Figs. 6 and 7 respectively. Analytical results are summarized in Fig. 8, in which given information from the IFE is also included for comparison.

Defect No. 7 on the calibration tube was not used for our analysis, because of its abnormality.

3. Testing

Testing on the test specimen was performed under the same conditions as used in the calibration tube with the encircling type coils.

To know the type of defects, the X-Y plotting was obtained from the scanning chart. Using the X-Y plottings, the defects were classified into groups. To determine the size, the detects in each group were compared with known defect from the calibration tube.

Obtained scanning chart is shown in Fig. 9, in which the sxial location of defect is included. The axial location was started from the opposite side of zero degree mark at azimuthal location.

The X-Y plotting sheets are shown in Fig. 10 for the frequency of

Signals X1, Y1, X2 and Y2 were filtered frequency eliminator at the last stage of electrical amplifiers. Range of frequencies of band path filter were between 5.8 and 12.0 Hz.

Signals X3 and Y3 were used to decide the defective location with large signals.

Two pairs of signal, (X1 Y1) and (X2, Y2) obtained from defects were vectorized to know the type of defect. These were shown in the form of X-Y plotting sheet respectively.

2.2 Method of calibration

Measuring equipment was calibrated with given calibration tube. Top of the calibration tube was set to opposite side of zero degree mark at azimuthal location.

The known defects on the calibration tube were measured by using the encircling type coils. Axial location of the defects measured were similar to those informed by the IFE. Type of the defects were identified by the phase angle, except the defect No. 7.

Results of scanning at the calibration tube are shown in Fig. 5. The X-Y plottings for known defects measured by the frequencies of 128 and 512 kHz, are shown in Figs. 6 and 7 respectively. Analytical results are summarized in Fig. 8, in which given information from the IFE is also included for comparison.

Defect No. 7 on the calibration tube was not used for our analysis, because of its abnormality.

3. Testing

Testing on the test specimen was performed under the same conditions as used in the calibration tube with the encircling type coils.

To know the type of defects, the X-Y plotting was obtained from the scanning chart. Using the X-Y plottings, the defects were classified into groups. To determine the size, the detects in each group were compared with known defect from the calibration tube.

Obtained scanning chart is shown in Fig. 9, in which the sxial location of defect is included. The axial location was started from the opposite side of zero degree mark at azimuthal location.

The X-Y plotting sheets are shown in Fig. 10 for the frequency of

128 kHz and Fig. 11 for 512 kHz, respectively.

To know the azimuthal location of defects, the probe type coils were also used. The probe type coils scanning were performed axially on the surface of the calibration tube and the test specimen at every nine degree.

4. Results and discussion

4.1 Estimation of defects by probe type coils

The azimuthal angles corresponded to defects are indicated in Table 1, together with those from the calibration tube.

As indicated in the table, five defects were determined from the measurement.

4.2 Estimation of defects by encircling type coils

i) Axial location:

The axial location of defects were estimated. These locations are indicated in Table 2, and also did in Fig. 9.

As indicated in both, fourteen defects were detected and numbered from the top.

ii) Type:

Figs. 12 and 13 are shown phase angle of each defect in the circular graph, concerning for frequency of 128 and 512 kHz with the calibration tube. Phase angles and type of defects are indicated in Table 3.

As indicated in the table, fourteen defects were classified in four groups.

According to the calibration, first group consisted of Nos. 1 to 4 were an internal circular groove. These phase angles were 329 - 340 degrees at the frequency of 128 kHz and 101 - 128 degrees at 512 kHz. Defect Nos. 1 to 4, however, were not identified as internal circular groove by the probe type coils. Furthermore, our experiences tell that there are no difference of phase angle among circular groove, scar and fatigue crack of internal. Defects in group were considered to be either internal scars or internal fatigue cracks informed by the IFE.

According to the calibration, second group consisted of Nos. 5 to 8 and 10 to 13 were an external scar. These phase angles were 307 - 322 degrees at the frequency of 128 kHz and 35 - 67 degrees

128 kHz and Fig. 11 for 512 kHz, respectively.

To know the azimuthal location of defects, the probe type coils were also used. The probe type coils scanning were performed axially on the surface of the calibration tube and the test specimen at every nine degree.

4. Results and discussion

4.1 Estimation of defects by probe type coils

The azimuthal angles corresponded to defects are indicated in Table 1, together with those from the calibration tube.

As indicated in the table, five defects were determined from the measurement.

4.2 Estimation of defects by encircling type coils

i) Axial location:

The axial location of defects were estimated. These locations are indicated in Table 2, and also did in Fig. 9.

As indicated in both, fourteen defects were detected and numbered from the top.

ii) Type:

Figs. 12 and 13 are shown phase angle of each defect in the circular graph, concerning for frequency of 128 and 512 kHz with the calibration tube. Phase angles and type of defects are indicated in Table 3.

As indicated in the table, fourteen defects were classified in four groups.

According to the calibration, first group consisted of Nos. 1 to 4 were an internal circular groove. These phase angles were 329 - 340 degrees at the frequency of 128 kHz and 101 - 128 degrees at 512 kHz. Defect Nos. 1 to 4, however, were not identified as internal circular groove by the probe type coils. Furthermore, our experiences tell that there are no difference of phase angle among circular groove, scar and fatigue crack of internal. Defects in group were considered to be either internal scars or internal fatigue cracks informed by the IFE.

According to the calibration, second group consisted of Nos. 5 to 8 and 10 to 13 were an external scar. These phase angles were 307 - 322 degrees at the frequency of 128 kHz and 35 - 67 degrees

at 512 kHz. According to our experiences, second group seems to be contained external scars unintentionally made some participant laboratories and fatigue cracks manufactured by the IFE. These detects were not distinguished, because the calibration tube had on fatigue crack.

According to the calibration, third group consisted of No. 9 was an external ridge. Its phase angles was 143 degree at the frequency of 128 kHz and 245 degree at 512 kHz.

According to the calibration, fourth group consisted of No. 14 was likely a through hole. Its phase angles was 328 degree at the frequency of 128 kHz and 81 degree at 512 kHz. In accordance with our experiences, defect No. 14 known from the signal with encircling type coils should be detect by the probe type coils. But it was not detected. In this place of the tube samples, signal from the probe type coils were rather reliable than the encircling type one. So the defect No. 14 was judged as noise.

iii) Dimension:

Volume of defect could not measure, because of the lack of sufficient numbers of the same type defects for making the calibration curve. So, the size of defects were estimated by the amplitude of the signal on the scanning chart. It was defined as $S = \sqrt{X^2+Y^2}$, where X and Y were maximum value of signal amplitude. Linear relationship between value S and defect volume is known according to the results of the first round robin test.

The estimated value, except for group 4, was compared with those from the calibration tube. The former was divided by the latter. The ratio is indicated in Tables 4 to 6 respectively according to the classified (internal circular groove, external scar and external ridge) group.

From the comparison, it can be said that the size of group 1 was ranged 0.8 - 1.3 to the known size of internal circular groove in the calibration tube. The size of group 2 was 0.04 - 0.07 to the external scar. The size of group 3 was 0.03 to the external ridge.

5. Conclusions

The eddy current testing equipment installed in Reactor Fuel Examination Facility, Tokai/ JAERI, can be used [1] to detect defects in the zircaloy tube samples, and [2] to estimate the axial location, the type and the relative dimension of defects by using the encircling type coils at 128 and 512 kHz frequencise respectively, and finally [3] to estimate the azimuthal location of defects by the probe type coils at 128 and 1024 kHz frequencies.

Concerning to the calibration tube, seven defects manufactured by Halden/ IFE were succeeded to detect the location and to provide as the standard type and size.

Concerning to the test specimen basing upon the comparison with the calibration tube, fourteen defects were detected and classified in four groups. They were (1) four internal circular groove, (2) eight external scar, (3) one external ridge and (4) one through hole. It should be mentioned, however, as has been discussed in the previous, we concluded group 1 should be either internal scar or fatigue crack and group 4 the noise.

In addition to the test specimen, the relative dimension were also determined.

Acknowledgments

The helpful discussions and cooperation obtained from Messrs. T. Kodama, Director of Department of Reactor Fuel Examination, F. Kanaizuka, and Y. Kanno, Chiefs of Fuel Examination Division and Dr. S. Kawasaki, Head of Fuel Reliability Laboratory 1 during the course of this analysis are gratefully acknowledged.

5. Conclusions

The eddy current testing equipment installed in Reactor Fuel Examination Facility, Tokai/ JAERI, can be used [1] to detect defects in the zircaloy tube samples, and [2] to estimate the axial location, the type and the relative dimension of defects by using the encircling type coils at 128 and 512 kHz frequencise respectively, and finally [3] to estimate the azimuthal location of defects by the probe type coils at 128 and 1024 kHz frequencies.

Concerning to the calibration tube, seven defects manufactured by Halden/ IFE were succeeded to detect the location and to provide as the standard type and size.

Concerning to the test specimen basing upon the comparison with the calibration tube, fourteen defects were detected and classified in four groups. They were (1) four internal circular groove, (2) eight external scar, (3) one external ridge and (4) one through hole. It should be mentioned, however, as has been discussed in the previous, we concluded group 1 should be either internal scar or fatigue crack and group 4 the noise.

In addition to the test specimen, the relative dimension were also determined.

Acknowledgments

The helpful discussions and cooperation obtained from Messrs. T. Kodama, Director of Department of Reactor Fuel Examination, F. Kanaizuka, and Y. Kanno, Chiefs of Fuel Examination Division and Dr. S. Kawasaki, Head of Fuel Reliability Laboratory 1 during the course of this analysis are gratefully acknowledged.

Table 1 Identification of azimuthal location of defects on the calibration tube and on the test specimen by probe type coils.

Zircaloy tube sample	Defect No.	Azimuthal Location (deg.)	Type of Defect Mentioned by IFE
Calibration tube	1	0 - 360	internal circular groove
	2	0 - 360	external ridge
	3a	0 - 360	external reduced wall
	3b		
	4	306 - 27	external scar (blind hole nearly flat bottomed)
	5	333 - 18	through hole
	6	315 - 27	through hole
	7	not estimated	internal scar
Test specimen	1	243 - 297	———
	2	162 - 207	
	3	54 - 99	
	4	297 - 360	
	5	180 - 207	
	6~14	not estimated	

Table 2 Identification of measured axial location of defects on the test specimen.

Defect No.	Axial Location (mm)	Defect No.	Axial Location (mm)
1	209	8	641
2	334.5	9	666.5
3	433.5	10	698
4	508.5	11	728.5
5	580	12	756
6	597	13	804.5
7	619.5	14	950

Table 3 Phase angle analysed by X-Y plotting data of defects on the test specimen.

Defect No.	Phase Angle (deg.)		Type of Defect Mentioned by IFE
	Freq. 128 kHz	Freq. 512 kHz	
1	340	128	internal circular groove
2	336	118	internal circular groove
3	331	103	internal circular groove
4	329	101	internal circular groove
5	318	60	external scar
6	316	67	external scar
7	322	62	external scar
8	322	63	external scar
9	143	245	external ridge
10	311	35	external scar
11	319	64	external scar
12	307	48	external scar
13	312	51	external scar
14	328	81	through hole

Table 4 Ratio of signals for defect No. 1-4 on the test specimen VS. signal for defect No. 1 (freq. 128 kHz; 0.61 V, freq. 512 kHz; 0.47 V) on the calibration tube.

Defect No.	Amplifier Gain (dB)	Signal Value (V)		Defect Signal Ratio		
		Freq. 128 kHz	Freq. 512 kHz	Freq. 128 kHz	Freq. 512 kHz	Average
1	-20	0.79	0.55	1.3	1.2	1.3
2	-20	0.50	0.37	0.8	0.8	0.8
3	-20	0.63	0.49	1.0	1.0	1.0
4	-20	0.47	0.40	0.8	0.9	0.9

Table 5 Ratio of signals for defect No. 5-8 and 10-13 on the test specimen VS. signal for defect No. 4 (freq. 128 kHz; 2.79 V, freq. 512 kHz; 3.26 V) on the calibration tube.

Defect No.	Amplifier Gain (dB)	Signal Value (V)		Defect Signal Ratio		
		Freq. 128 kHz	Freq. 512 kHz	Freq. 128 kHz	Freq. 512 kHz	Average
5	-10	0.18	0.25	0.06	0.08	0.07
6	-10	0.17	0.21	0.06	0.06	0.06
7	-10	0.16	0.18	0.06	0.06	0.06
8	-10	0.20	0.20	0.07	0.06	0.07
10	-10	0.07	0.15	0.03	0.05	0.04
11	-10	0.12	0.14	0.04	0.04	0.04
12	-10	0.11	0.23	0.04	0.07	0.06
13	-10	0.15	0.22	0.05	0.07	0.06

Table 6 Ratio of signal for defect No. 9 on the test specimen VS. signal for defect No. 2 (freq. 128 kHz; 7.14 V, freq. 512 kHz; 13.49 V) on the calibration tube.

Defect No.	Amplifier Gain (dB)	Signal Value (V)		Defect Signal Ratio		
		Freq. 128 kHz	Freq. 512 kHz	Freq. 128 kHz	Freq. 512 kHz	Average
9	-10	0.20	0.22	0.03	0.02	0.03

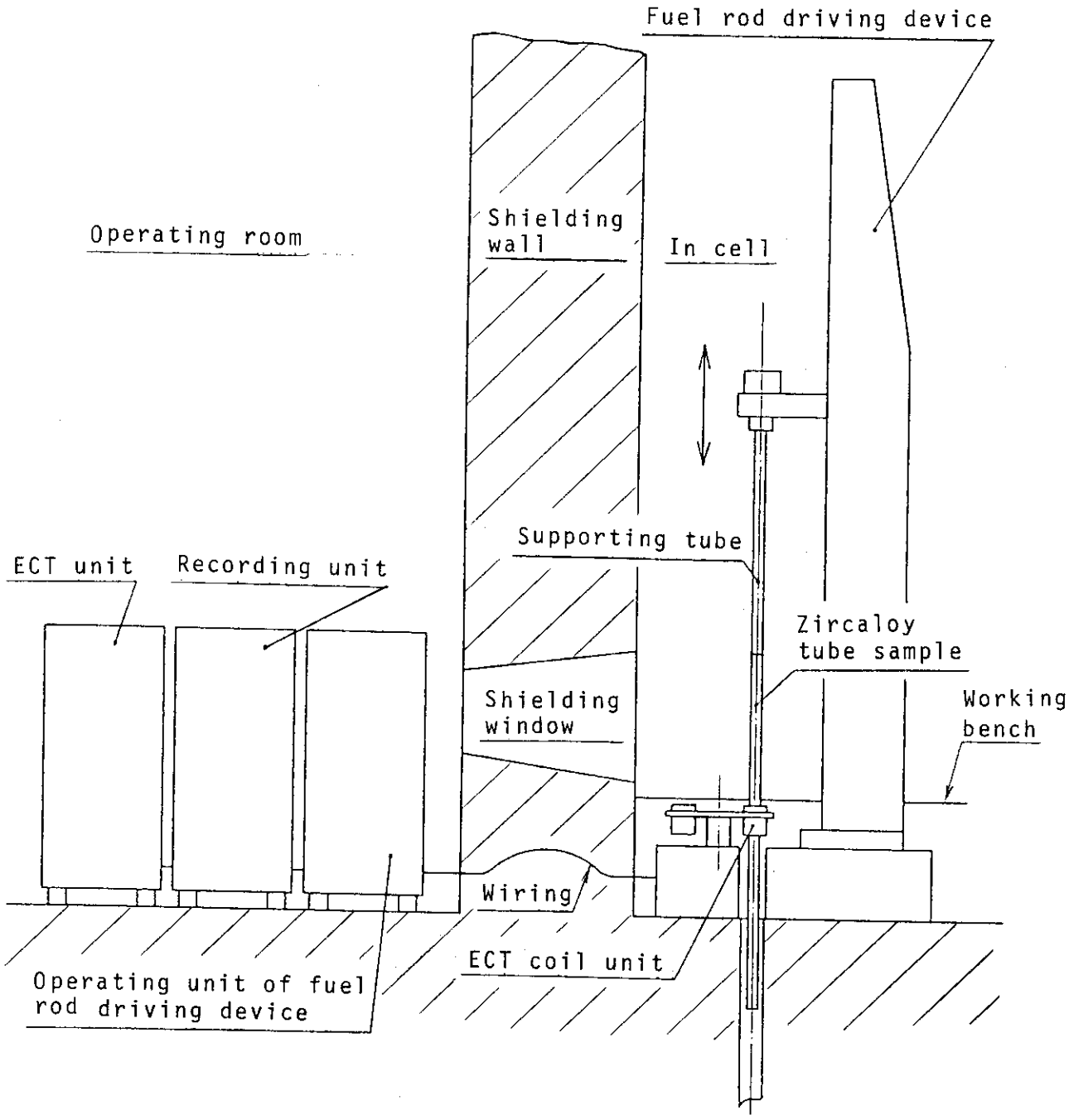

Fig. 1 Outline of multifrequency eddy current testing (ECT) system.

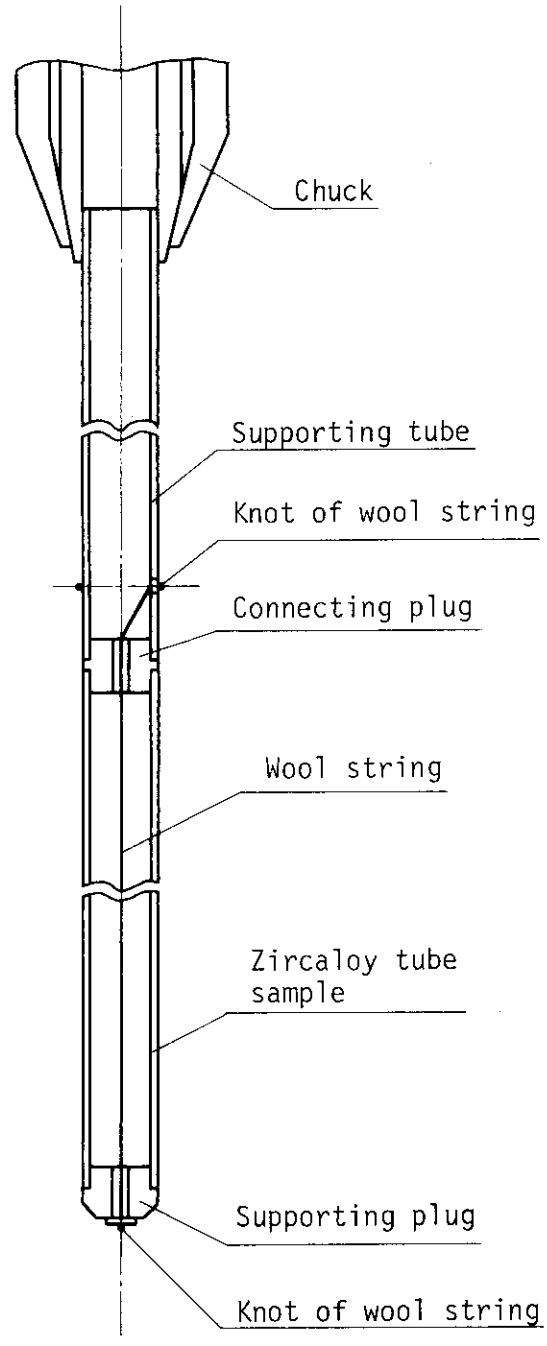

Fig. 2 Details of supporting tube and zircaloy tube sample.

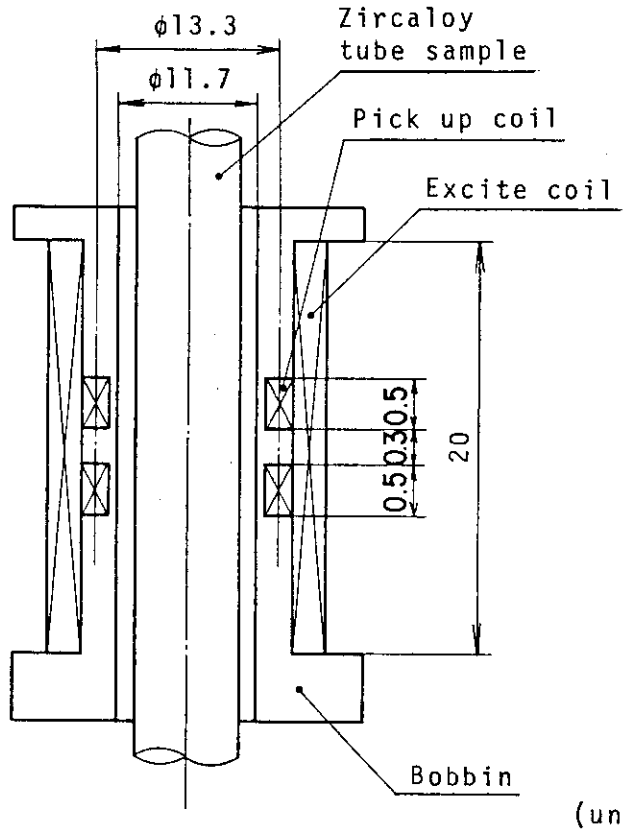

Fig. 3 Encircling type eddy current testing coils.

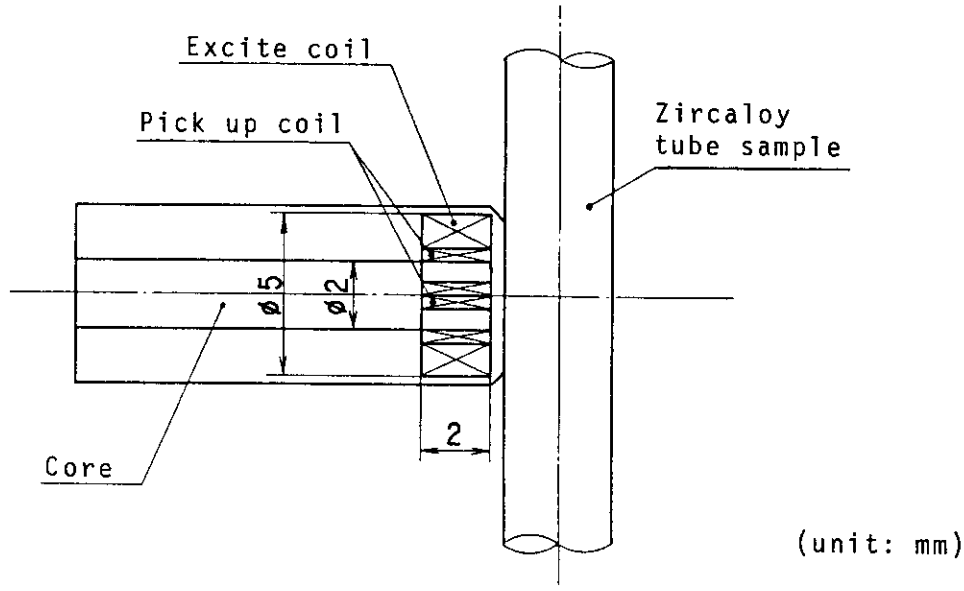

Fig. 4 Probe type eddy current testing coils.

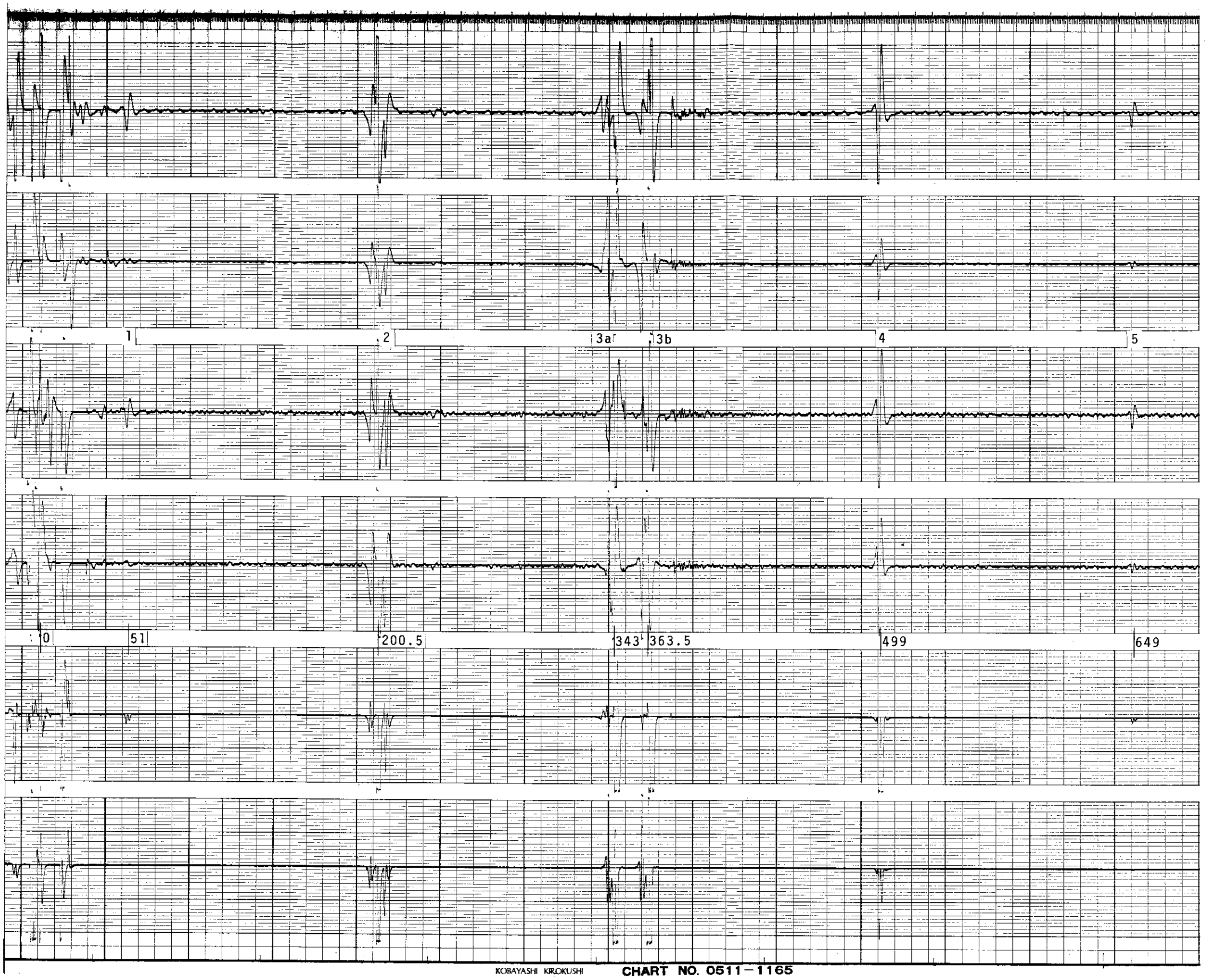

Fig. 5 Scanning data of the calibration tube. (part 1) (amplifier gain : -20 dB)

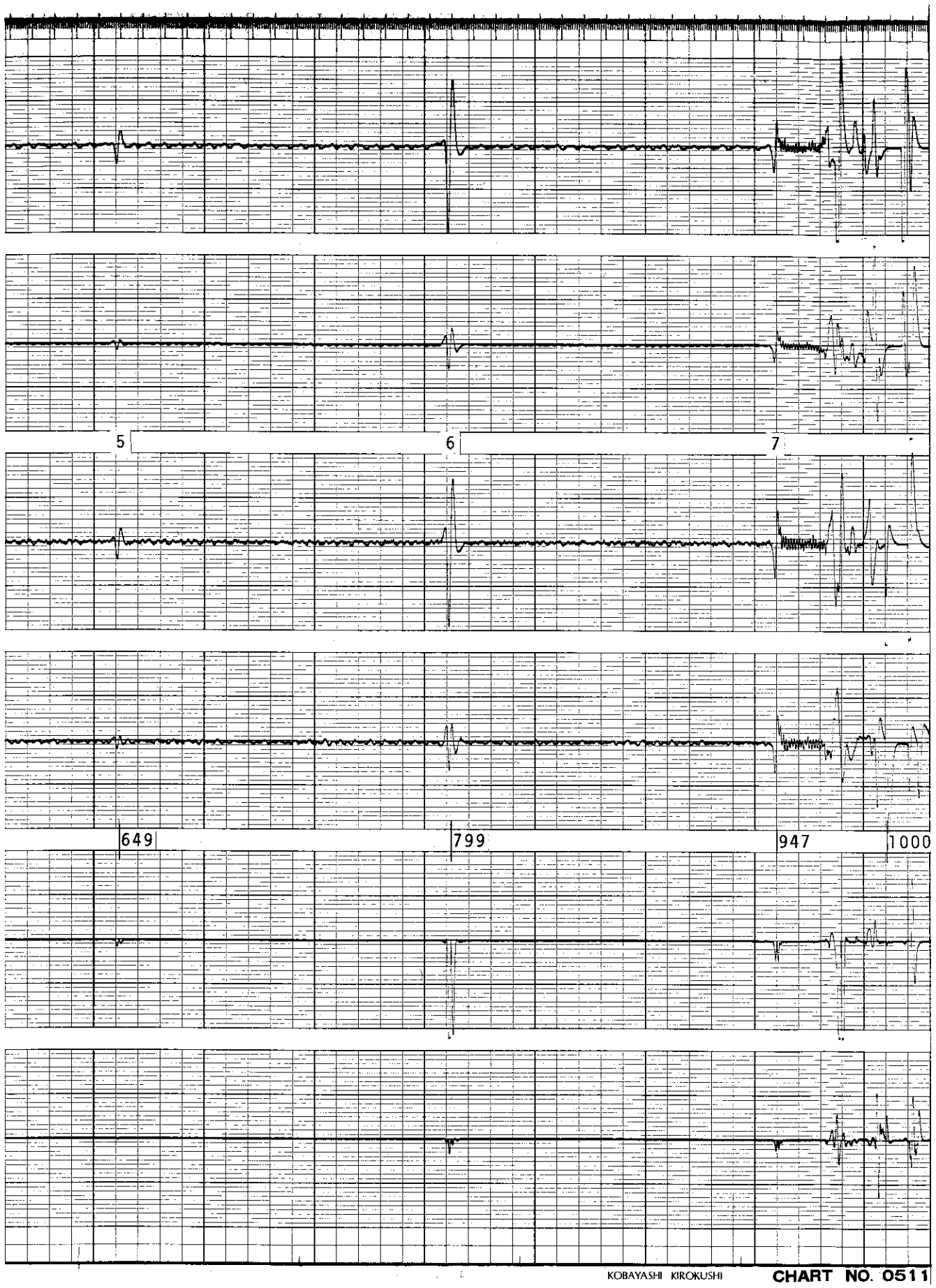

Fig. 5 Scanning data of the calibration tube. (part 2) (amplifier gain : -20 dB)

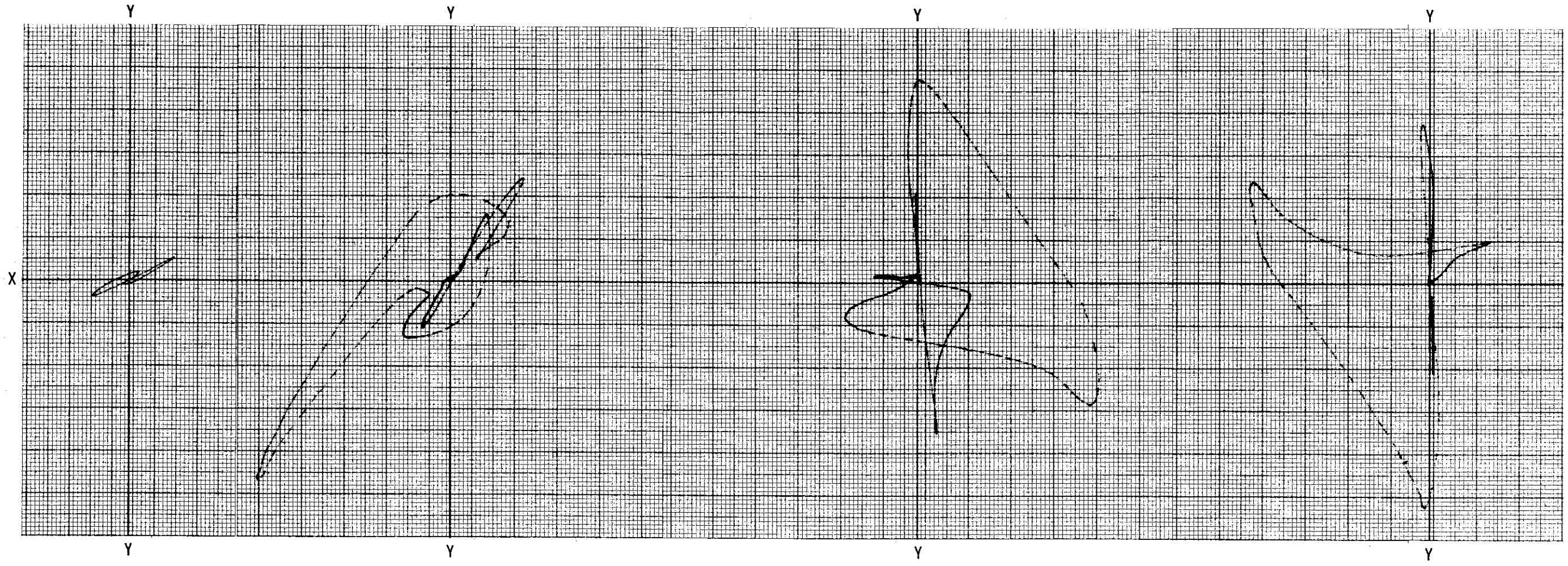

(1) Defect No. 1　(2) Defect No. 2　(3) Defect No. 3a　(4) Defect No. 3b

Fig. 6 X-Y plotting data of defect at frequency 128 kHz on the calibration tube. (part 1)
(amplifier gain : -20 dB)

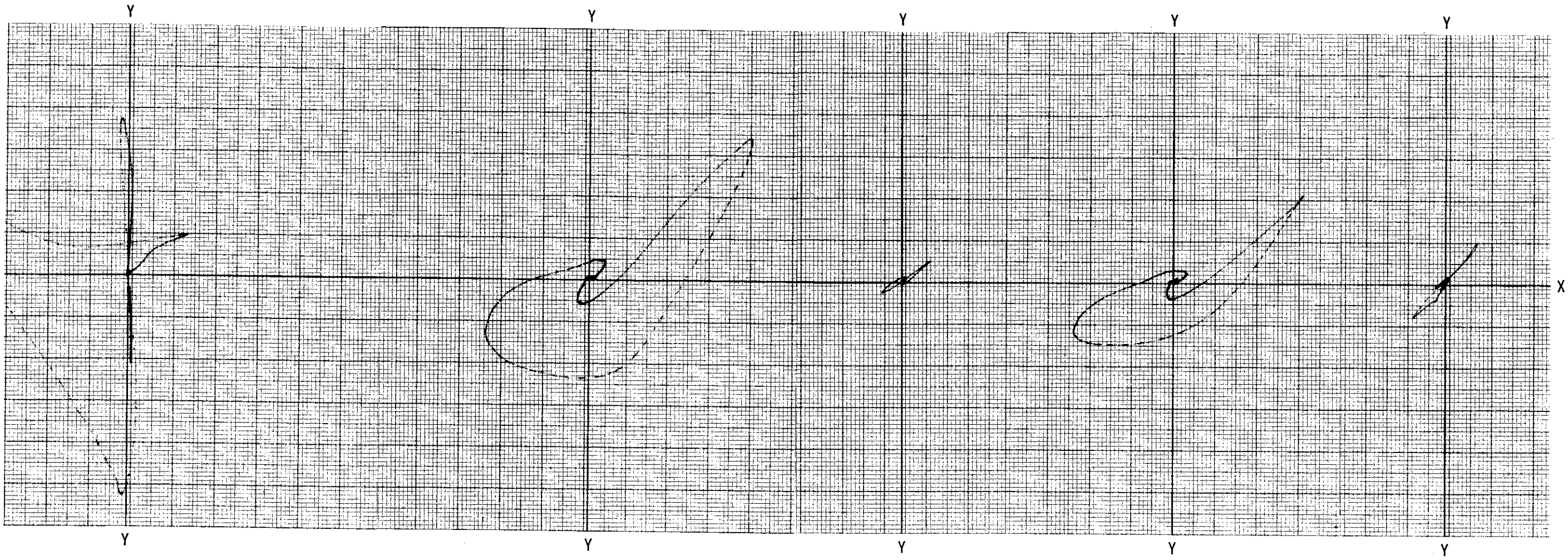

(4) Defect No. 3b (5) Defect No. 4 (6) Defect No. 5 (7) Defect No. 6 (8) Defect No. 7

Fig. 6 X-Y plotting data of defect at frequency 128 kHz on the calibration tube. (part 2)
(amplifier gain : -20 dB)

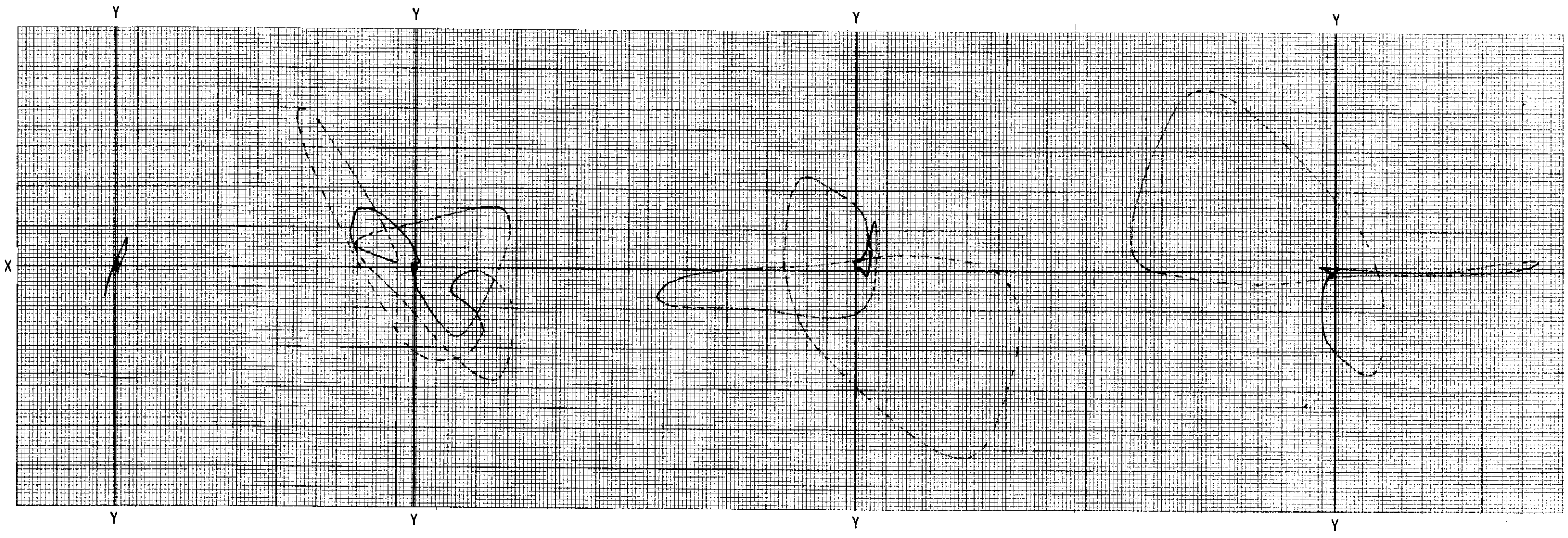

(1) Defect No. 1 (2) Defect No. 2 (3) Defect No. 3a (4) Defect No. 3b

Fig. 7 X-Y plotting data of defect at frequency 512 kHz on the calibration tube. (part 1)
(amplifier gain : -20 dB)

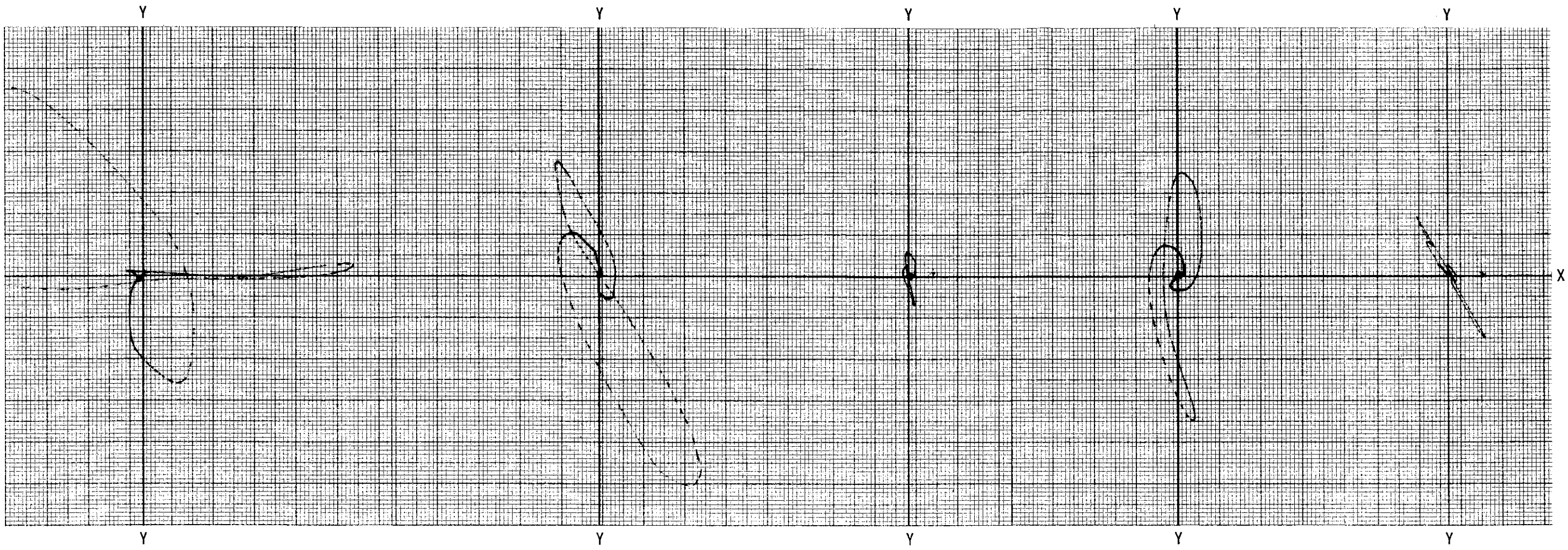

(4) Defect No. 3b (5) Defect No. 4 (6) Defect No. 5 (7) Defect No. 6 (8) Defect No. 7

Fig. 7 X-Y plotting data of defect at frequency 512 kHz on the calibration tube. (part 2)
(amplifier gain : -20 dB)

Defect No.		1	2	3	4	5	6	7
Information from IFE	Axial Position (mm)	50	200	350	500	650	800	950
	Type of Defect	internal circular groove	external ridge	external reduced wall	external scar (blind hole nearly flat bottomd	through hole	through hole	internal scar
Our Result	Axial Location (mm)	51	200.5	(3a) 343 (3b) 363.5	499	649	799	947
	Phase Angle (deg.) Freq. 128 kHz	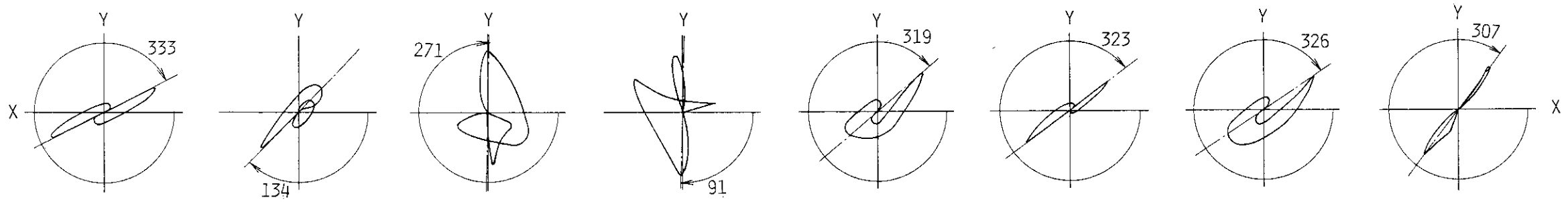						
	Freq. 512 kHz	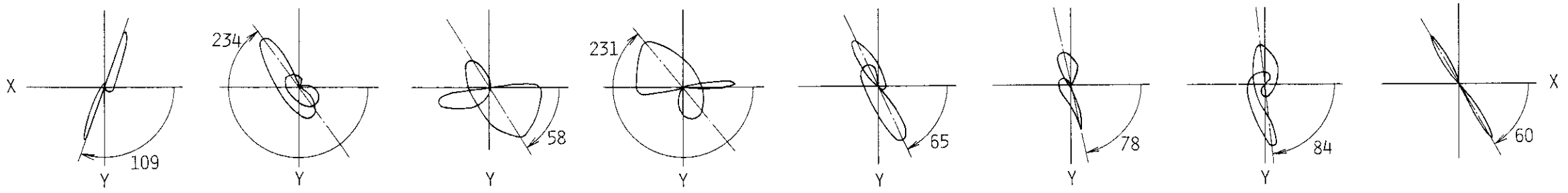						

Fig. 8 Comparison of artificial defect of information from IFE and our result on the calibration tube.

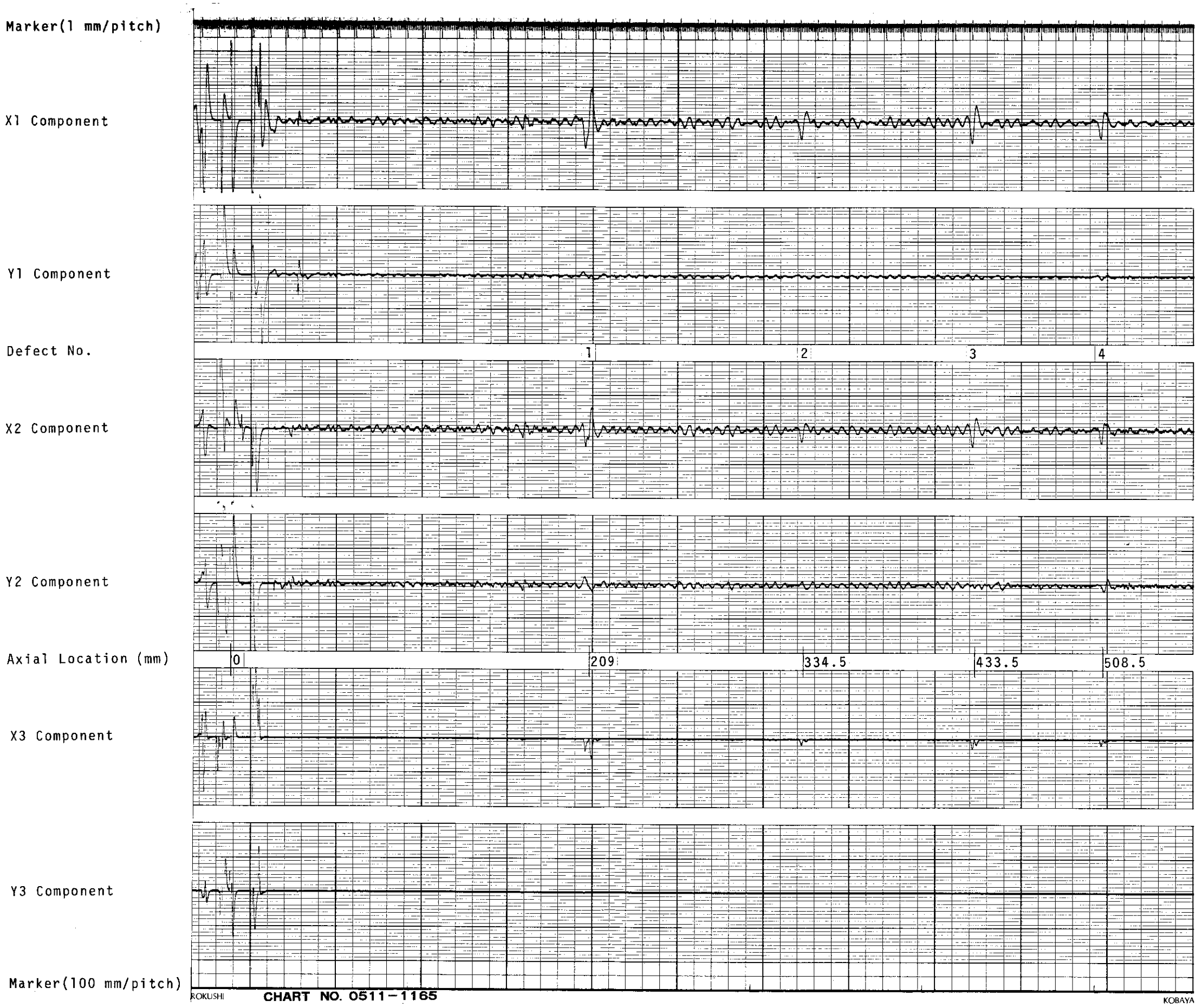

Fig. 9 Scanning data of the test specimen. (part 1) (amplifier gain : -20 dB)

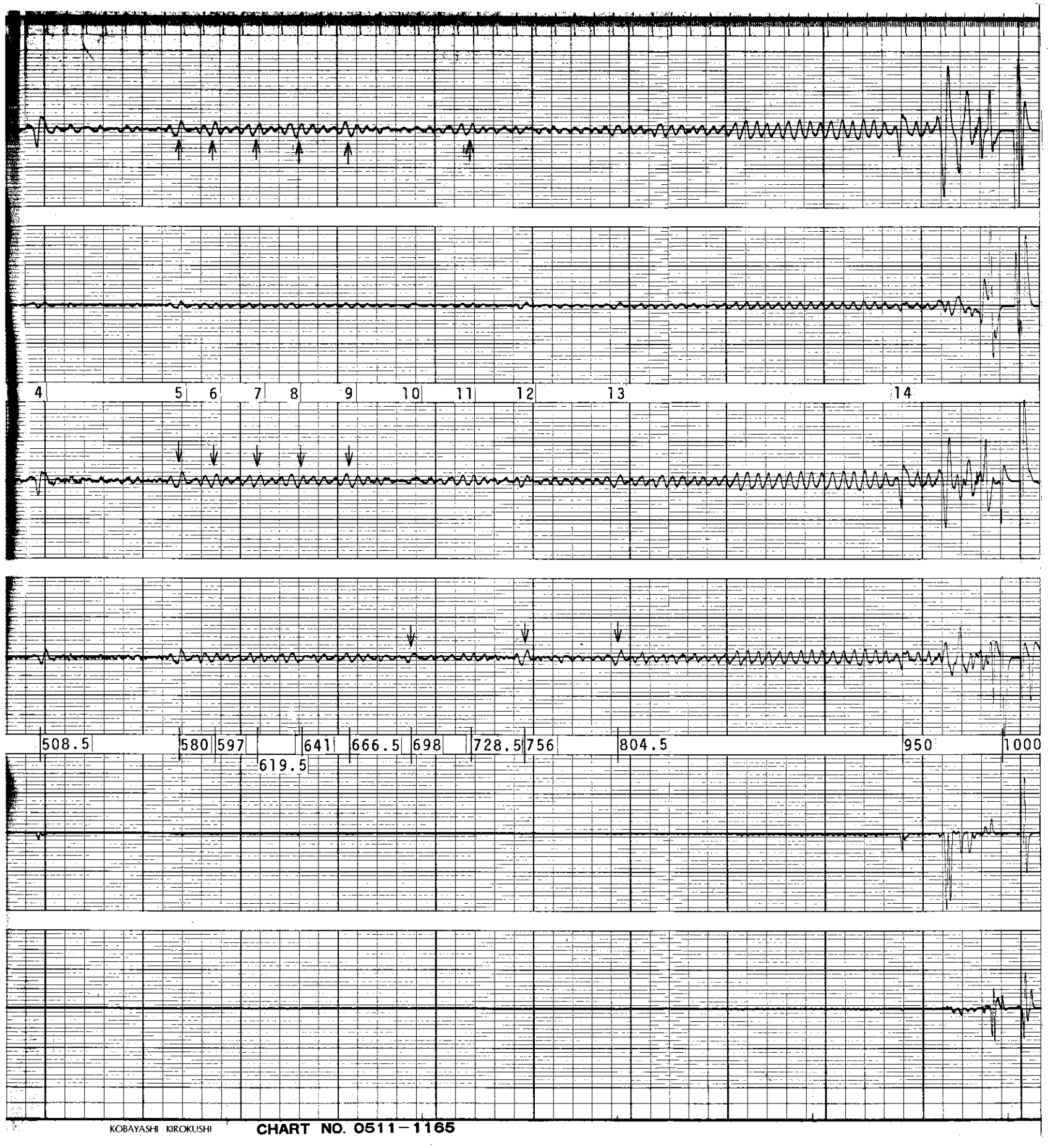

Fig. 9 Scanning data of the test specimen. (part 2) (amplifier gain : -20 dB)

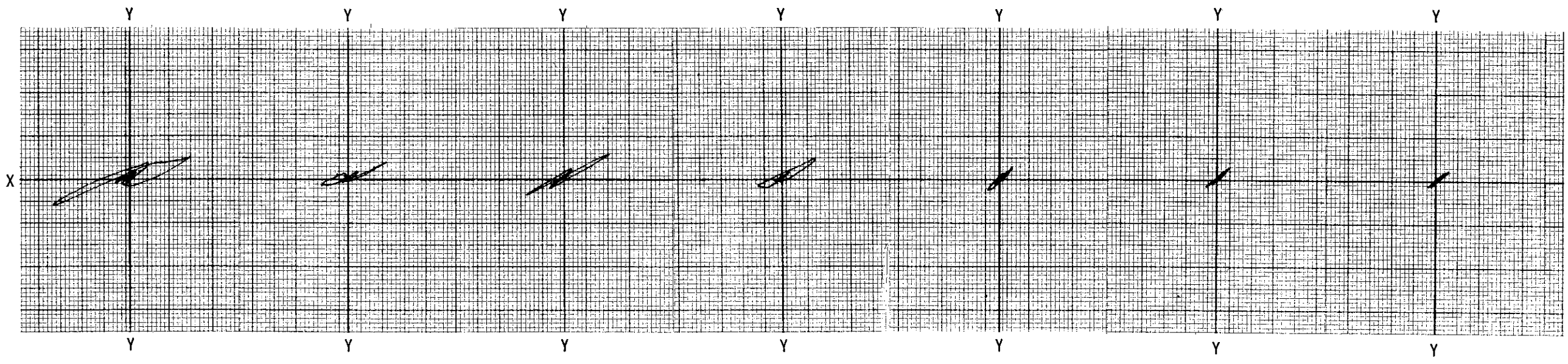

(1) Defect No. 1 (2) Defect No. 2 (3) Defect No. 3 (4) Defect No. 4 (5) Defect No. 5 (6) Defect No. 6 (7) Defect No. 7

Fig. 10 X-Y plotting data of defect at frequency 128 kHz on the test specimen. (part 1)
(amplifier gain : -20 dB)

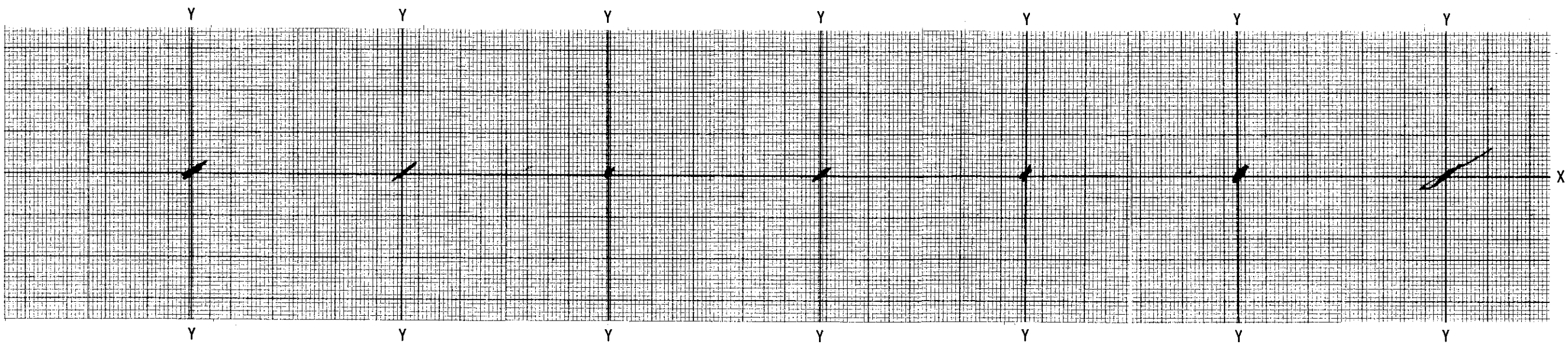

No. 7 (8) Defect No. 8 (9) Defect No. 9 (10) Defect No. 10 (11) Defect No. 11 (12) Defect No. 12 (13) Defect No. 13 (14) Defect No. 14

Fig. 10 X-Y plotting data of defect at frequency 128 kHz on the test specimen. (part 2)
(amplifier gain : -20 dB)

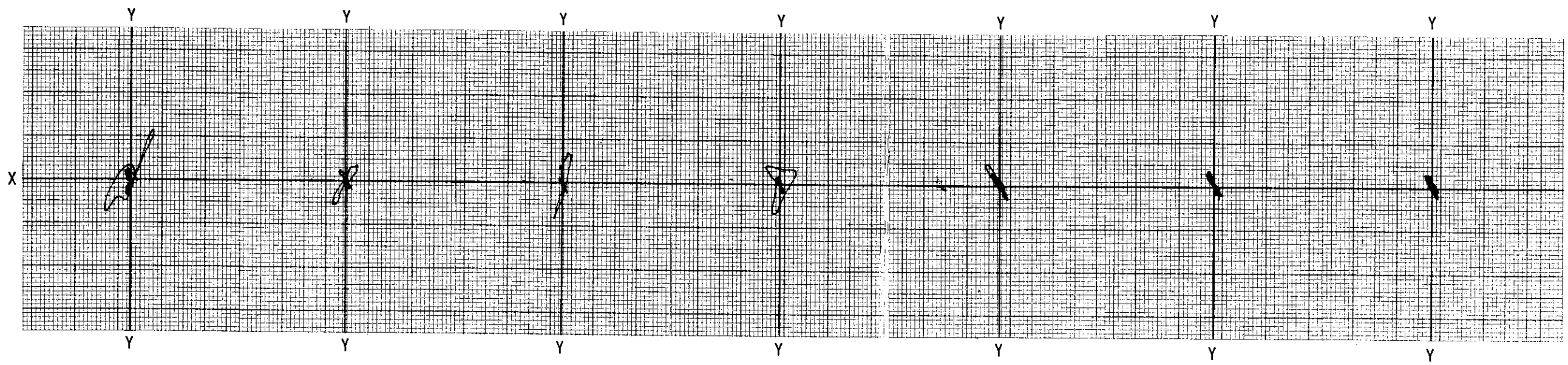

(1) Defect No. 1 (2) Defect No. 2 (3) Defect No. 3 (4) Defect No. 4 (5) Defect No. 5 (6) Defect No. 6 (7) Defect No. 7

Fig. 11 X-Y plotting data of defect at frequency 512 kHz on the test specimen. (part 1)
(amplifier gain : -20 dB)

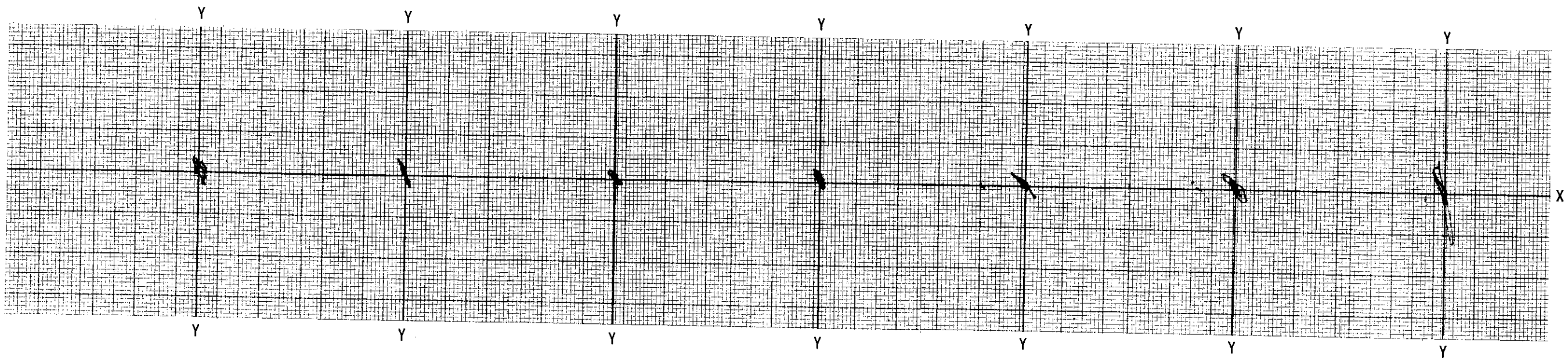

No. 7 (8) Defect No. 8 (9) Defect No. 9 (10) Defect No. 10 (11) Defect No. 11 (12) Defect No. 12 (13) Defect No. 13 (14) Defect No. 14

Fig. 11 X-Y plotting data of defect at frequency 512 kHz on the test specimen. (part 2)
(amplifier gain : -20 dB)

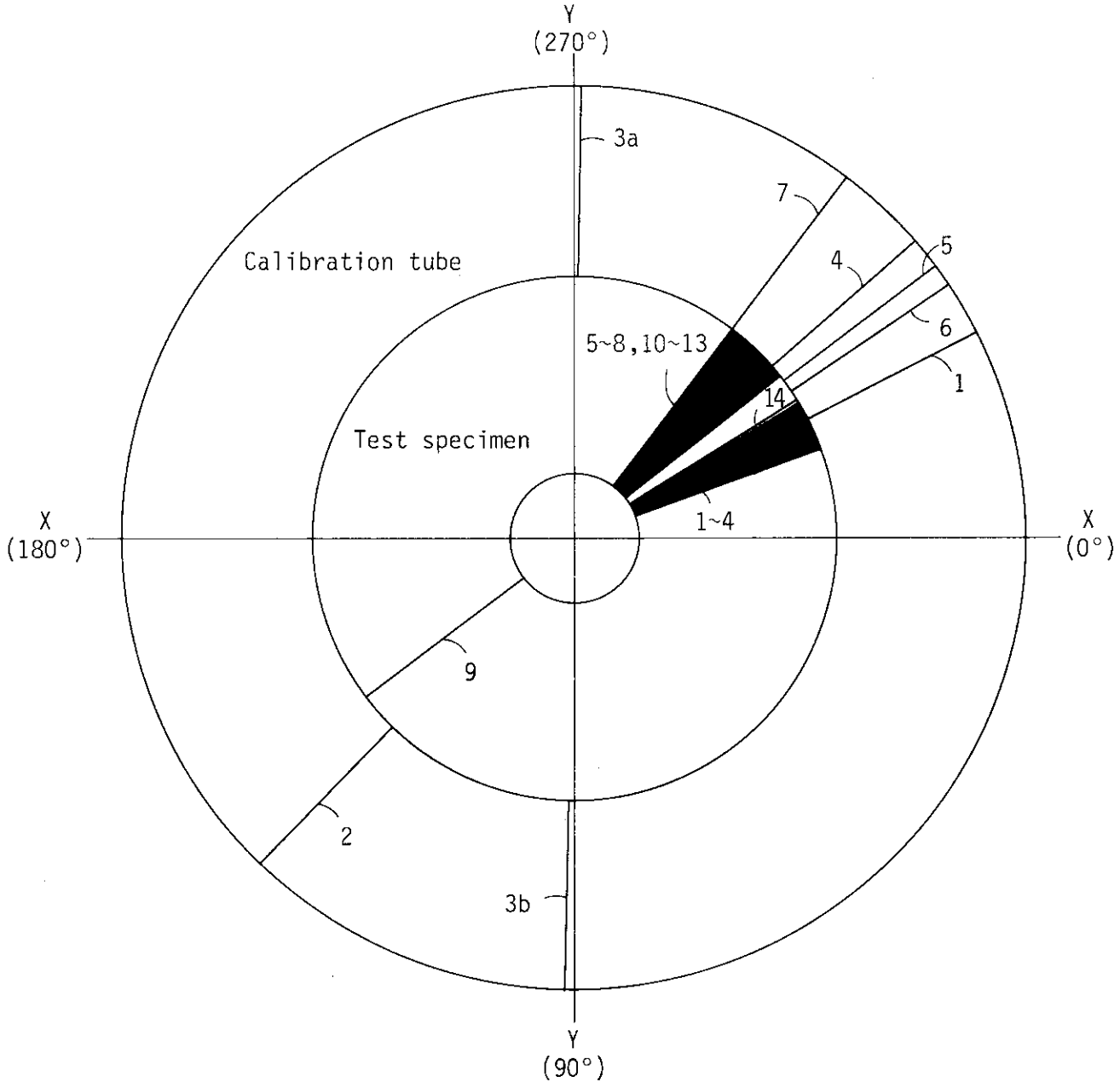

Note; A number on figure is shown number of defect.

Fig. 12 Relationship between type of defect and signal phase angle at frequency 128 kHz.

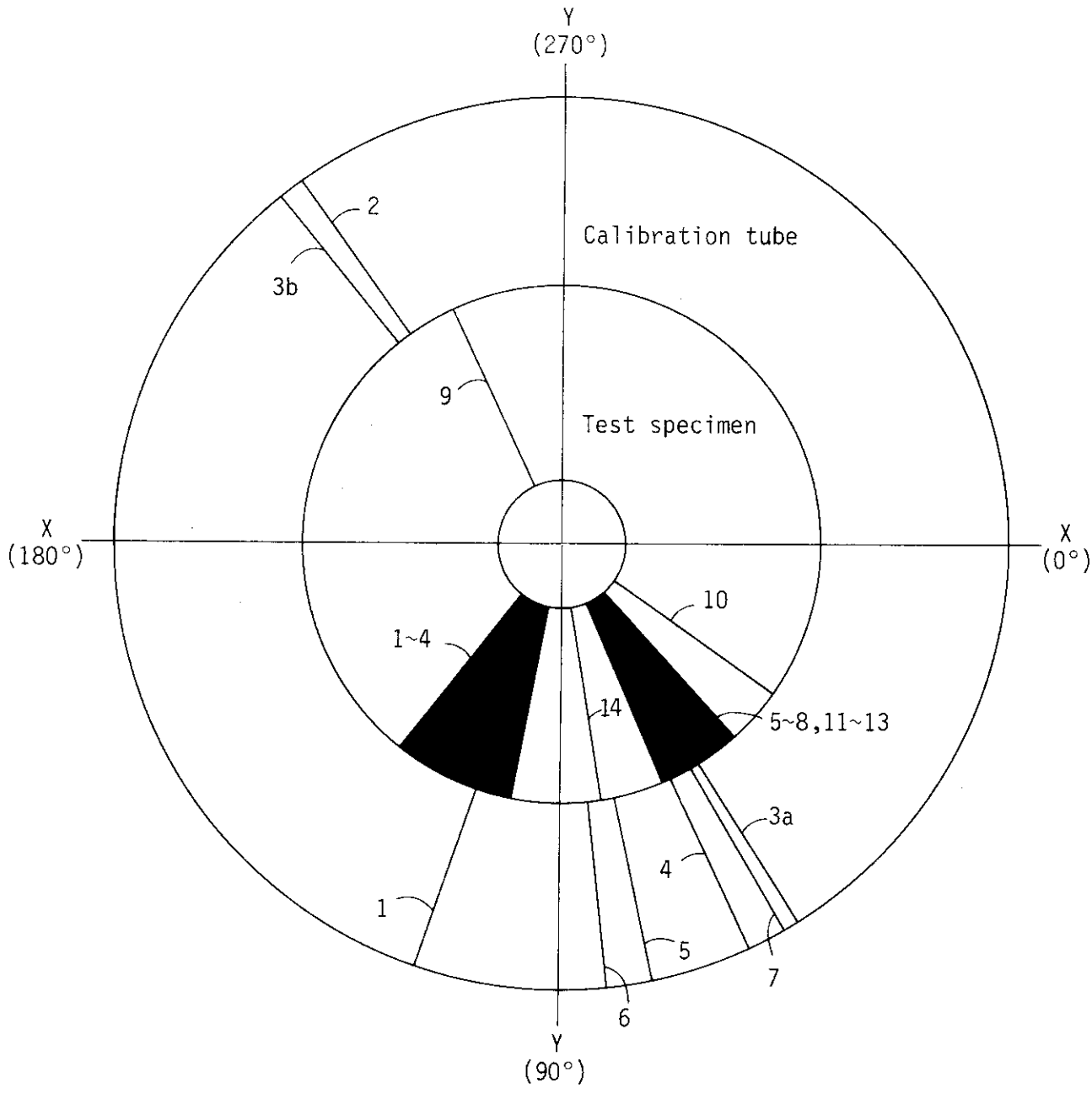

Note; A number on figure is shown number of defect.

Fig. 13 Relationship between type of defect and signal phase angle at frequency 512 kHz.